

**Separation of green solvent dimethyl carbonate/methanol azeotropic mixture by  
pervaporation with polydimethylsiloxane/polyhedral oligomeric silsesquioxane composite  
membrane**

Wenhai Lin<sup>1\*</sup>, Qin Li<sup>2</sup>, Chuanwen Lin<sup>1</sup>, Dingding Xiang<sup>3</sup>, Dongzhi Chen<sup>4</sup>, Huan wang<sup>1</sup>, HuajunZu<sup>1</sup>

<sup>1</sup> Hefei University

<sup>2</sup>China Energy Engineering Group Anhui Electric Power DesignInstitute Co., Ltd

<sup>3</sup> School of Chemistry and Chemical Engineering, Qiannan Normal University for Nationalities

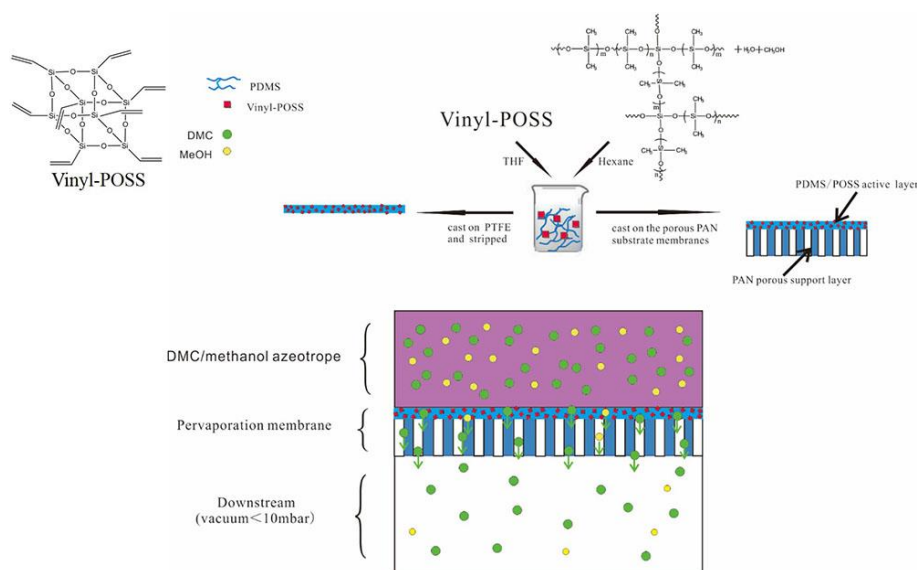
<sup>4</sup> School of Materials Science and Engineering, Wuhan Textile University

\*Corresponding author: Wenhai Lin

E-mail: (*linwenhai@whu.edu.cn*), tel: +86 18605653201

ACCEPTED MANUSCRIPT

## GRAPHICAL ABSTRACT



## ABSTRACT

A composite active layer was prepared by cage-type polyhedral oligomeric silsesquioxane (POSS) and polydimethylsiloxane (PDMS) and was combined with polyacrylonitrile (PAN) porous support layer to form pervaporation (PV) membrane, which was used in the PV membrane separation of dimethyl carbonate (DMC)/methanol (MeOH) azeotrope. The active layer of PDMS/POSS was characterized by using X-ray diffraction, thermogravimetry, and swelling test, and the PV membrane was characterized by using scanning electron microscope and contact angle measurement. The permeability flux, separation factor and swelling/diffusion selectivity of the composite membrane were evaluated by PV test. Results show that POSS interferes with the ordered structure of PDMS, reduces the contact angle of the membrane, and is conducive to the preferential penetration of DMC. The separation flux of DMC was greatly increased in the PV process of DMC/MeOH azeotropic mixture. Moreover, the excellent swelling selectivity of PDMS/POSS active layer kept the separation factor at a high level. The novelty of this research is that POSS nanoparticles modified PV composite membranes, which can be used to separate DMC/MeOH azeotropic mixtures with good results. The maximum permeation flux of composite membrane M-3 was  $4.9\text{ kg/m}^2\text{h}$  at the operating temperature of  $50\text{ }^\circ\text{C}$ , and the separation factor was 2.31, which was higher than data reported in literature.

**Keywords:** Polyhedral oligomeric silsesquioxane, Composite membrane, Azeotropic mixture separation, Pervaporation, Swelling selectivity

## 1. Introduction

Cage polyhedral oligomeric silsesquioxane (POSS), which has a general structure of  $(\text{RSiO}_{1.5})_n$ , is a typical nanoparticle. POSS with  $n = 8$  is the silica with the smallest cage-like nanostructure in diameter. Chemical functional groups can be added to the side chain extending around the cage-like structure to provide the special performance required for application scenarios. In recent years, POSS, as a kind of nano silica with high consistency, regular structure, and adjustable function, has been widely concerned in the field of organic–inorganic composite modification [1-3]. POSS has excellent compatibility with PDMS and has attracted wide attention in the field of high-end silicone rubber in recent years [4]. The organic-inorganic composite modified silicone rubber membrane prepared by PDMS/POSS composite material has high performance and high durability [5].

Organic-inorganic composite membrane pervaporation separation (PV) is a hotspot in the field of azeotropic mixture separation in recent years [6,7]. Azeotropic/extractive distillation method easily introduces third-party impurities, and the energy consumption is high. Membrane separation method has attracted the attention of researchers because of its unique advantages [8]: this method can achieve efficient separation of azeotropes under mild conditions and has the advantages of no pollution, space saving, and low energy consumption. The separation principle involves the difference in the affinity between components in azeotropic mixture and the liquid side surface of membrane material, the difference in diffusion rate through membrane, and the difference in evaporation and separation rate from the downstream surface of membrane. This mechanism allows a component to pass through membrane at a faster speed, whereas the passing speed of the other component is limited. Therefore, the introduction of the membrane as a third-party interaction medium can break the interaction effect between the two components of azeotrope to achieve efficient separation.

The research work introduced POSS with hydrophobic structure to improve the performance of PV membrane in different polarity azeotropic mixture. On the one hand, POSS can further increase the nonpolarity of the membrane and prevent high polarity components escaping from the downstream surface of the membrane; on the other hand, POSS, as a special cage-like nanoparticles (Fig. 1), will change the microstructure of the membrane when dispersed in the polymer chain segment of PDMS. POSS can increase the diffusion ability of low polarity components and may increase the membrane permeation flux while maintaining a high separation factor.

PDMS/POSS composite membrane has good industrial application prospects for PV separation of DMC/MeOH azeotrope. Dimethyl carbonate (DMC) was registered in Europe as a nontoxic or slightly toxic chemical product in 1992[9,10]. DMC is being widely used to replace highly toxic carbonylation raw materials of phosgene ( $\text{COCl}_2$ ) to synthesize the intermediates of carbamate, polycarbonate, isocyanate, and other polymer synthetic materials [11,12]. DMC can also be used as an environmentally friendly and green methylation reagent to replace dimethyl sulfate (DMS) and  $\text{CH}_3\text{Cl}$ , which are highly toxic and corrosive. At the same time, DMC can be used as an additive for gasoline antiknock and reduce VOC content in exhaust gas by replacing MTBE, which may pollute groundwater [13,14]. DMC additive can effectively improve the conductivity of the electrolyte of lithium battery, form a passivation membrane on the anode surface, improve the stability of the battery, and extend the service life of the battery [15]. In addition, DMC is also a clean, safe, and excellent organic solvent, which is widely used in medicine and coating industry[16,17]. Therefore, DMC is often referred to as the "new cornerstone" of organic synthesis in the 21st century.

The main methods of DMC synthesis that have been industrialized and applied in a large scale are methanol oxidative carbonylation, urea alcoholysis, and direct synthesis of carbon dioxide and MeOH [18-20]. These methods have the advantages of cheap raw materials, high DMC yield, little environmental harm, and relatively mild and safe synthesis conditions, but all the production processes are equilibrium reactions. The unreacted MeOH will form high polarity/low polarity azeotropic mixture with DMC. Azeotropic temperature under normal pressure is  $64\text{ }^\circ\text{C}$ , and the

azeotropic group is composed of 70 wt.% MeOH and 30 wt.% dimethyl carbonate [21]. Therefore, the azeotropic mixture of DMC and MeOH cannot be separated by a simple distillation column. The most commonly used separation method in the industry is the pressurized distillation method, but its equipment is expensive; a safety accident will cause serious losses [22,23]. Therefore, finding a safe and low-cost alternative process for azeotropic separation is important. Low-temperature crystallization method can obtain DMC with high purity but has a large energy consumption and a complex process. At present, the use of this method is only limited to the manufacture of high-purity DMC for batteries with high added value [24].

Pervaporation (PV) membrane separation technology has been widely concerned by researchers in the field of DMC/MeOH azeotrope separation. At present, silicotungstic acid hydrate/chitosan [25], polyacrylic acid/polyvinyl alcohol (PVA)[8,26], zeolite/chitosan[27], chitosan/silica [28], chitosan hollow fiber membranes[29], polyamide-6[30], perfluoro-ion-exchange membranes[31], PVA-perfluorosulfonic acid/PAN composite membranes[32], nanotuned pore SiO<sub>2</sub> membranes[21], and other membrane materials have been used in PV membrane separation of DMC/MeOH system. Most of these membrane materials have been used in other PV systems for dehydration and for MeOH priority permeation in DMC/MeOH system. However, some problems, such as the high (70 wt.%) total MeOH content in azeotropic mixture, have been found in the application process. For example, a large amount of MeOH needs to be evaporated when combined with ordinary distillation. The hydrogen bond between MeOH molecules increases the latent heat of evaporation by almost 3 times that of DMC (1073:381 kJ/mol) [33], which deviates from the original intention of low energy consumption in PV process. However, the efficiency of MeOH preferentially permeating through the membrane will decrease rapidly with decreasing MeOH content. At the same time, the excessive swelling of hydrophilic polymer caused by MeOH at a certain temperature (40 - 70 °C) will also affect the long-term stability of the membrane.

Based on the above reasons, researchers have begun to look for PV membranes that preferentially penetrate DMC. PDMS has stable thermodynamic properties, good durability, and good hydrophobic

and lipophilic properties and will have higher mechanical stability after filling with nano silica [34, 35]. In recent years, researchers have studied the PV of PDMS membrane filled with various surface-modified nano-SiO<sub>2</sub> and verified that it has the performance of preferentially passing DMC [12, 36,]. The novelty of the research is that the PDMS/POSS composite membranes are used to separate DMC/MeOH azeotropic mixtures. It opens a new path for the application of POSS nanoparticles to modify pervaporation membranes to separate high-polarity/low-polarity azeotropic mixtures in PV. High-value DMC preferentially through PV film to better meet the requirements of industrial applications. In order to explore the pervaporation mechanism of PDMS/POSS composite membrane, the influence of process parameters on PDMS/POSS PV membrane have been studied.

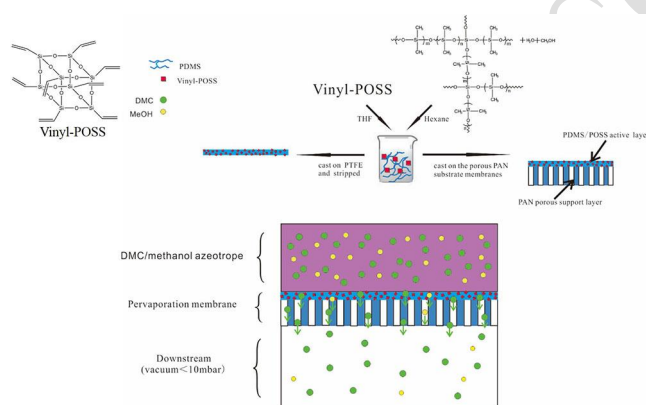


**Figure 1.** Construction of PDMS/POSS membrane and its application in DMC/MeOH azeotrope PV separation

## 2. Materials and methods

### 2.1. Materials

MeOH, dimethyl carbonate, n-hexane, and tetrahydrofuran were purchased from Sinopharm Chemical Reagent Co., Ltd. (analytical reagent). PAN (retention molecular weight  $5 \times 10^4$ ) porous ultrafiltration membrane was purchased from Hangzhou Water Treatment Technology Development Center.  $\alpha,\omega$ -Dihydroxypolydimethyl siloxane (36,000 molecular weight) and tetramethoxysilane (99%) were purchased from Hubei Wuda Organosilicon New Material Co., Ltd., and 101 # organic tin mixture curing catalyst was purchased from Hubei Wuda Photonics Technology Co., Ltd. Vinyl-POSS [4] was self-made in the laboratory.

## *2.2. Preparation of pure PDMS solution and PDMS/POSS composite solution*

A certain amount of  $\alpha,\omega$ -dihydroxypolydimethyl siloxane was placed into a flask and weighed. An appropriate amount of n-hexane was added, and the mixture was stirred at room temperature for 4 h and allowed to stand for filtration to obtain  $\alpha,\omega$ -dihydroxypolydimethyl siloxane with a concentration of 5 wt.% solution. A certain amount of vinyl-POSS was weighed into a flask and added with an appropriate amount of tetrahydrofuran, and the mixture was stirred at room temperature for 4 h. After filtration, a vinyl-POSS tetrahydrofuran solution having a concentration of 5 wt.% was prepared. Vinyl-POSS tetrahydrofuran solution and  $\alpha,\omega$ -dihydroxypolydimethyl siloxane solution were mixed in a certain ratio and added with a certain amount of cross-linking agent tetramethylsilane (the ratio is the total mass of 10%  $\alpha,\omega$ -dihydroxypolydimethyl siloxane). The total solid masses are called M-1, M-2, and M-3 according to the vinyl-POSS added amount of 5 wt.%, 15 wt.%, and 30 wt.%, respectively, and the group without vinyl-POSS solution is called M-0. The mixtures were placed in conical flasks and stirred at 25 °C for 4 h. Finally, a certain amount of 101 # organic tin catalyst is added and stirred for 5 min to obtain PDMS/POSS casting membrane composite solution.

## *2.3. Preparation of PDMS/POSS active layer and complex PV membranes for test*

The production process of the active layer used for testing the properties, such as swelling, is as follows: the mixed cast membrane solution was coated on the surface of a clean tetrafluoroethylene board placed horizontally, dried at room temperature in a dust-free and air convection room, placed in a vacuum drying box at 60 °C for 4 h, and then removed for use. The manufacturing process of the membrane for testing PV performance is as follows: the PAN porous support membrane was immersed in 5% sodium hydroxide aqueous solution at 50 °C for 1 h, then washed to neutral with deionized water, immersed in 1 N hydrochloric acid solution at room temperature for 20 min, and rinsed with deionized water until neutral. The PAN porous support membrane was fixed on a flat and clean glass plate. A certain mass of PDMS/POSS casting membrane solution was weighed and poured on the treated PAN support layer, and the entire glass plate was horizontally placed in a dust-free air convection room and allowed to stand at room temperature to dry. The glass plate was placed in a

vacuum drying box at 60 °C for 4 h and then cooled to room temperature to obtain a PDMS/POSS-modified silicone rubber PV membrane. Pure PDMS contrast PV membrane was prepared by the same process.

#### 2.4. Swelling experiments

Equilibrium swelling experiments of pure PDMS active layer and PDMS/POSS active layer were performed at 30 - 50 °C. First, the dry membrane was weighed as  $W_D$ , then immersed in a DMC/MeOH azeotrope or pure DMC or pure MeOH in a constant temperature-sealed container, and swelled to equilibrium after 24 h. The liquid on the surface of the membrane was quickly wiped out, and the membrane was weighed; the weighing mass was  $W_S$ . The time interval from the removal to the completion of weighing was within 5 s. Equation (1), which was used to calculate the swelling degree  $D_S$ , is as follows [37]:

$$D_S = \frac{W_s - W_d}{W_d} \quad (1)$$

All experiments were performed at least three times, and the results were averaged.

Sorptivity  $\alpha_S$  was calculated using Equation 2:

$$\alpha_S = \frac{D_{SD} / D_{SM}}{F_D / F_M} \quad (2)$$

$D_{SD}$  and  $D_{SM}$  are the swelling degree of the active layer in DMC and MeOH, respectively.  $F_D$  and  $F_M$  are the mass of DMC and MeOH in the azeotrope, respectively. Sorptivity results show the interaction of the active layer with DMC and MeOH molecules and the change in the interaction between DMC and MeOH molecules due to the active layer.

#### 2.5. X-ray diffraction analysis(XRD)

The active layer film prepared according to the method in 2.2 was dried under an infrared lamp and was spread flat on the fixture of a Shimadzu XRD-6000 diffractometer (Japan), and the XRD measurement conditions were selected for graphite monochrome  $\text{CuK}\alpha$  radiation ( $\lambda = 1.54060 \text{ \AA}$ ) at



40 kV/30 mA. The scanning diffraction angle range of 5° to 60° and scanning rate of 4°/min were used to identify the difference in the ordered structure in the active layer film.

#### 2.6. Thermogravimetric analysis(TG)

About 5 – 10 mg of the active layer film prepared according to the method in 2.2 was cut out and placed in an Al<sub>2</sub>O<sub>3</sub> crucible. Scanning was performed using a SETSYS 16 instrument (France) at a heating rate of 10 °C/min. Samples were placed in nitrogen atmosphere with flow rate of 50 ml/min, and the temperature range was 20 °C to 600 °C.

#### 2.7. Scanning electron microscopy(SEM)

The PDMS/POSS PV membrane prepared according to the method in 2.2 was broken under liquid nitrogen cooling, and the surface was coated with a layer of sputtered gold. The surface/section morphology of the membrane was examined through the FEI Quanta 200 (Holland) scanning electron microscope.

#### 2.8. Contact angle experiment

Contact angle experiment was performed through a DSA100 instrument (Kruss Company, Germany) with a high-speed camera observation system for droplet angle. The static contact angle of 5 µl of DMC/MeOH azeotrope on the membrane surface was measured by the static sessile drop method to determine the azeotropic affinity of pure PDMS and PDMS/POSS PV membrane surfaces. The membranes to be tested were vacuum dried before testing. The measurement time was less than 10 s to reduce the effect of evaporation. Equation (3) was used to calculate the contact angle  $\theta$  [38]:

$$\theta = \cos^{-1} \frac{\cos\theta_a + \cos\theta_r}{2} \quad (3)$$

$\theta_r$  is the receding angle, and  $\theta_a$  is the advancing angle. The final result of the contact angle is the average calculated after repeating all experiments at least three times.

#### 2.9. PV experiments

PV experiments were performed in the temperature range of 30 – 50 °C. The gas chromatograph was calibrated by accurately preparing multiple concentrations of a DMC/MeOH mixture, and then

the composition of the liquid feed mixture was analyzed and supplemented in an appropriate amount to keep the composition constant. The PV test began when the system was stable. Permeated steam from the downstream side was collected in a cold well immersed in liquid nitrogen tank (the internal air pressure was 1 mm Hg), and collection time interval was fixed. The cold wells were collected, sealed, and warmed to room temperature to weigh, and the permeate flux was calculated. Gas chromatography was used to determine the DMC content in the permeate. Gas chromatograph SP3400 (China) with a FID detector and a 2 m × 6 mm PEG-20M capillary column was used. The test column temperature was 170 °C, and the carrier gas was nitrogen at a flow rate of 30 ml/min. All PV experimental results were calculated by averaging the experimental results repeated four times, and the average standard deviation was less than 10%.

Equations (4) and (5) were used to calculate the permeate flux and separation factor to evaluate the separation performance of pure PDMS and PDMS/POSS PV membranes:

$$\alpha = \frac{y_D / y_M}{x_D / x_M} \quad (4)$$

$$J = \frac{W}{At} \quad (5)$$

where J is the permeate flux,  $\alpha$  is the separation factor, W (g) is the weight of the permeate, A (m<sup>2</sup>) is the effective membrane area, t (h) is the operation time,  $y_D/y_M$  is the mole fraction ratio of DMC and MeOH in the permeate, and  $x_D/x_M$  is the mole fraction ratio of DMC and MeOH in the feed.

### **3. Results and Discussion**

#### *3.1. Membranes characterization*

##### *3.1.1. XRD analysis*

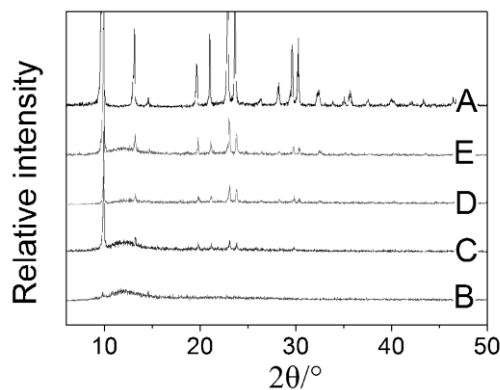


**Figure 2.** XRD patterns of pure vinyl-POSS (A), pure PDMS active layer M-0 (B), and PDMS/POSS composite PV active layers M-1 (C), M-2 (D), and M-3 (E)

The X-ray diffraction patterns of pure PDMS and PDMS/POSS active layers are shown in Fig. 2. The pure PDMS active layer has a distinct single peak between  $5^\circ$  and  $20^\circ$ , and the peak top is about  $12^\circ$  (Fig. 2 B). Fig. 2 A shows the X-ray diffraction pattern of pure vinyl-POSS, which shows a sharp peak at  $2\theta = 9.8^\circ, 13.0^\circ, 19.5^\circ, 21.0^\circ, 22.8^\circ, 23.6^\circ,$  and  $29.6^\circ$ . Sharp peaks found everywhere proves that vinyl-POSS is a highly crystalline compound [4]. The peaks around  $12^\circ$  become shorter and flatter with increasing amount of POSS added when PDMS and POSS were combined, and each characteristic peak of POSS is still obvious. This result shows that the ordered structure of PDMS is affected by POSS, and the ordered structure of PDMS/POSS composite active layer decreases with increasing amount of POSS added. The active layer has more pathways for small molecules to pass through, and each characteristic peak of POSS is completely preserved. This finding shows that POSS still maintains its own cage structure after the formation of the composite active layer. The PV process has special effects on DMC and MeOH molecules and affected the PV results.

### 3.1.2. TG analysis

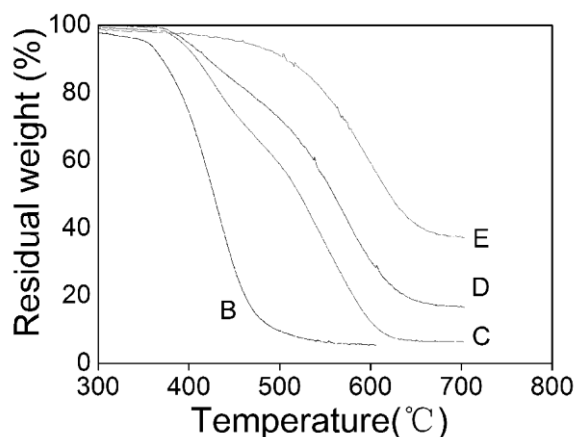


**Figure 3.** TGA results of pure PDMS (B) and PDMS/POSS composite PV active layers M-1(C), M-2(D), M-3(E)

Fig. 3 shows the thermal decomposition curves of pure PDMS and PDMS/POSS active layers. The thermal stability of the membranes is  $M-3 > M-2 > M-1 > M-0$ . The thermal decomposition process of PDMS was hindered and the thermal resistance of the composite was improved with increasing POSS content compared with the thermal decomposition curve of pure PDMS. POSS is generally believed to be a stable cage silica particle dispersed in PDMS that hinders the thermal movement of PDMS polymer chain segment and delays the thermal decomposition process. However, POSS needs extra energy to destroy the cage structure by thermal decomposition. Another secondary reason is that POSS particles are dispersed in PDMS, and the network structure formed in the thermal decomposition process prevents the outward diffusion of thermal decomposition products, such as volatile gases, and also hinders the thermal decomposition reaction [5].

### 3.1.3. SEM analysis

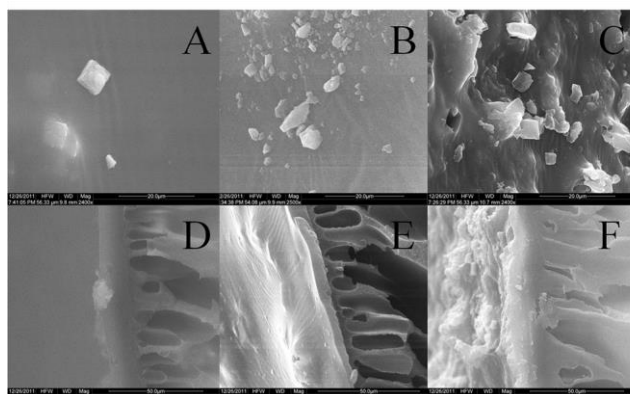


**Figure 4.** Morphologies of PDMS/POSS composite PV membranes M-1 (A surface, D cross-section), M-2 (B surface, E cross-section), and M-3(C surface, F cross-section)

As shown in Figs. 4A–F, the surface roughness of PDMS/POSS composite membrane increased with increasing POSS content, and the crystal structure of POSS remained completely in the inner and surface of the membrane. The rough membrane surface is conducive to the separation of the permeation components from the membrane surface, and POSS in the membrane, which will cause a large number of pores for the permeation components to pass through, has a positive effect on the increase in the PV flux. The combination of POSS and PDMS was close, the membrane surface was compact and continuous, and some adherent POSS crystals occasionally appeared when the content of POSS was relatively low (5 wt.%). A large number of spaces formed around POSS crystals and crystals can be observed on the surface of PDMS when the content of POSS increases to 30 wt.%. In the past, we used to study the surface and cross section of pure PDMS through SEM. The surface of the membrane is flat and dense, and the cross section shows that no obvious holes and phase separation interface in the membrane [5]. The difference between PDMS/POSS composite membrane and pure PDMS composite membrane in PV performance is determined by their surface and internal structures.

#### 3.1.4. Contact angle analysis

**Table 1.** Contact angles of DMC/MeOH azeotrope on pure PDMS and PDMS/POSS composite PV membranes

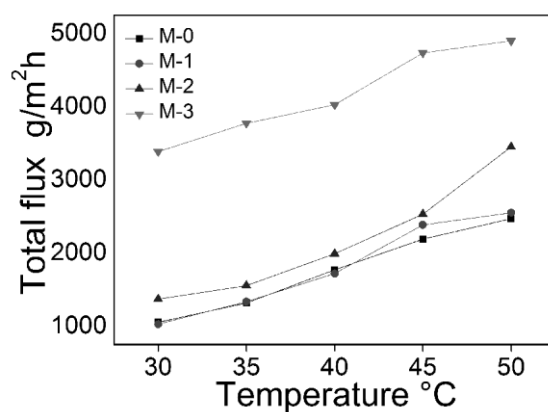
| Membrane | Proportion (wt.%) |            | Contact angle(° ) |
|----------|-------------------|------------|-------------------|
|          | PDMS              | Vinyl-POSS |                   |
| M-0      | 100               | 0          | 39 ± 1            |
| M-1      | 95                | 5          | 34 ± 1            |
| M-2      | 85                | 15         | 28 ± 1            |
| M-3      | 70                | 30         | 11 ± 1            |

The contact angle test results of pure PDMS and PDMS/POSS PV membrane are shown in Table 1. The data show that the contact angle of DMC/MeOH azeotrope on the membrane surface decreased gradually with the addition of POSS; hence, small molecules are easier to dissolve into the surface of the composite membrane. SEM and XRD patterns show that the POSS wrapped in PDMS membrane

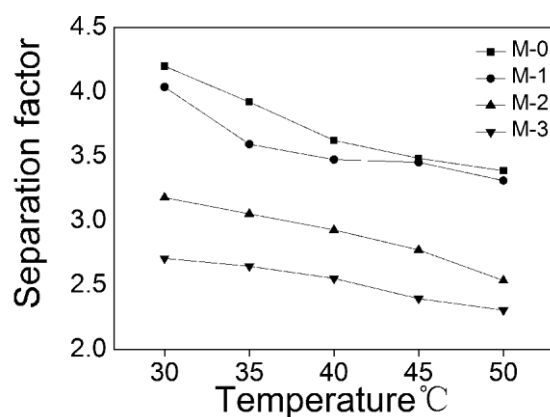
seriously interfered with the ordered structure of PDMS when PDMS and POSS formed the membrane together. POSS crystals or voids were present on the surface of the composite membrane and made the membrane rough and undulating, which is different from the smooth and compact surface of pure PDMS. In addition, POSS has hydrophobic groups extending outwards that further reduce the contact angle. The results show that the composite membrane became more conducive to the solubilization of small molecules on the liquid side of the feed in the PV process than the pure PDMS membrane with increasing POSS content.

### 3.2. PV characteristics

#### 3.2.1. Test of PV performance of PDMS/POSS composite membrane



**Figure 5.** Flux of PV for DMC/MeOH azeotrope in pure PDMS membrane and PDMS/POSS composite PV membranes at different temperatures



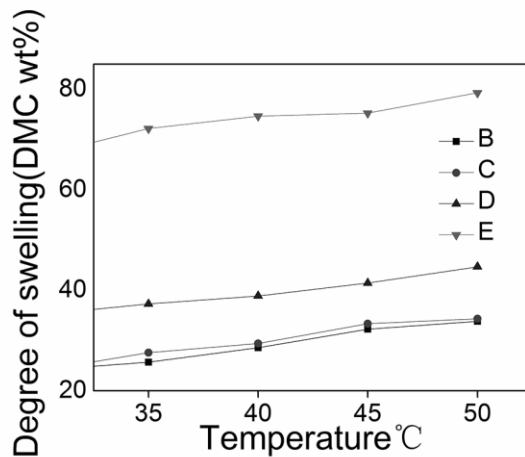
**Figure 6.** Separation factor of PV for DMC/MeOH azeotrope in pure PDMS membrane and PDMS/POSS composite PV membranes at different temperatures

Fig.5 and fig.6 show that the permeation flux of PDMS/POSS composite membrane is significantly increased and the separation factor is decreased compared with pure PDMS membrane. As a kind of nano silica particles, POSS enters into the chain segment of PDMS to form a gap between the two phases. These voids are conducive to the transfer of small molecules in the membrane and reduce the permeability resistance of small molecules. Another reason is that the addition of POSS destroys the ordered structure of PDMS (Fig. 2). The polarity of PDMS, which is very small and has a blocking effect on MeOH with strong polarity, is conducive to DMC penetration [12, 34]. The SEM figure (Fig. 4) shows that the structure with high roughness was left in the PDMS as the content of POSS increased and greatly increased the free volume inside the active layer, enabled MeOH molecules to pass through the membrane quickly, and thus reduced the separation factor. Fig. 6 shows that the flux increased greatly and the separation factor decreased greatly when the content of POSS increased to 30% because this effect becomes more obvious. However, most of the permeated through DMC, which indicates that PDMS/POSS composite membrane is suitable for DMC/MeOH azeotropic mixture to preferentially PV through DMC.

Fig. 5 and fig.6 show that the flux of pure PDMS membrane and PDMS/POSS composite membrane increases when the temperature increases due to the acceleration of polymer segment motion and the increase in the free volume inside the membrane [31]. The separation factor decreases with the increase of temperature, because the increase of temperature will accelerate the movement of MeOH molecules, and the increase rate of the saturated vapor pressure of MeOH exceeds the increase rate the saturated vapor pressure of DMC. At 30°C, the saturated vapor pressure of MeOH is 21.76Kpa, the saturated vapor pressure of DMC is 10.77 KPa, MeOH:DMC has a saturated vapor pressure ratio of 2.02. This ratio gradually increases with increasing temperature. At 60°C, the saturated vapor pressure of MeOH is 84.53Kpa, the saturated vapor pressure of DMC is 34.56 KPa,

MeOH:DMC has a saturated vapor pressure ratio of 2.44[39, 40]. Therefore, the corresponding separation factor decreases when the temperature increases.

### 3.2.2. Analysis of swelling degree and sorptivity/diffusivity of PDMS/POSS active layers



**Figure 7.** Degree of swelling in the DMC of pure PDMS and PDMS/POSS composite PV active layers at different temperatures

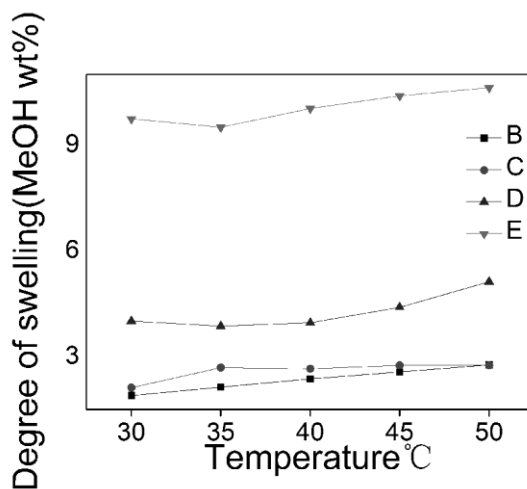


**Figure 8.** Degree of swelling in the MeOH of pure PDMS and PDMS/POSS composite PV active layers at different temperatures

Fig.7 and fig.8 shows the swelling curve of PDMS/POSS active layer in DMC and MeOH. The DMC swelling degree and MeOH swelling degree of PDMS/POSS active layer increased with increasing temperature.



The general explanation is that the rise in the temperature accelerates the movement of the permeate molecules and increases the tendency to enter the membrane. At the same time, the increase in the temperature of the membrane itself accelerates the movement of the internal polymer chain segment and expands the free volume; therefore, the swelling degree increases when the temperature rises. The swelling degree increased with increasing POSS content because POSS breaks the ordered structure between the molecular segments of PDMS, increases the free volume, and has more voids between them that can hold DMC and MeOH molecules. Therefore, the swelling degree increases when the content of POSS increases. The swelling degree of MeOH and DMC suddenly increased when the loading amount of POSS reached 30%. According to SEM, the morphology of the active layer exceeded the critical point when the loading amount of POSS reached 30% due to the increase in porosity. Swelling experiments show that POSS is a hydrophobic nanosilica, and its addition increases the swelling degree of PDMS membrane. For all PDMS/POSS active layers, the swelling degree of DMC is higher than that of MeOH. Hence, our membrane is the first to swell DMC.

The calculation of diffusion selectivity  $\alpha_D$  is calculated using Eq. 6:

$$\alpha_D = \frac{\alpha}{\alpha_S} \quad (6)$$

where  $\alpha$  is the separation factor, and  $\alpha_S$  is the sorptivity factor [34].

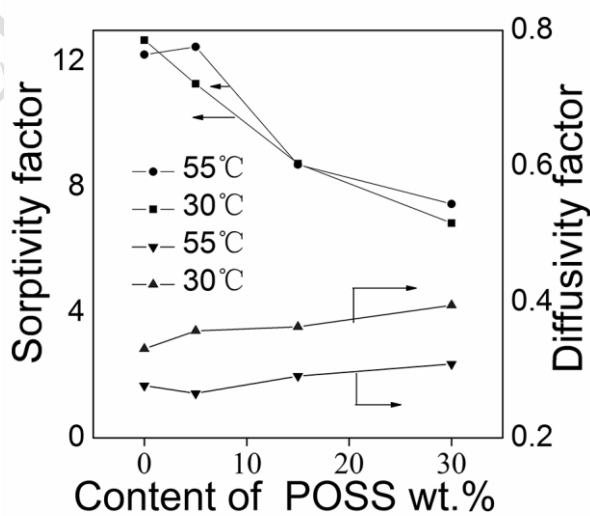


**Figure 9.** Comparison of adsorption and diffusion selection performance of composite PV active layers with different POSS contents

The effect of POSS content on the sorptivity and diffusivity of PDMS/POSS active layer is shown in Fig. 9. The gradual decrease in sorptivity when POSS content increased may be caused by the increase in the free volume in the composite membrane due to the addition of POSS. MeOH can cause more swelling into the composite membrane, thereby decreasing the sorptivity. However, the free volume without selectivity increased and sorptivity decreased with increasing amount of POSS. Sorptivity represents the trend of the thermodynamic selectivity of the membrane.

However, the slight increase in diffusivity with the addition of POSS is attributed to the fact that the ability of DMC to pass through the membrane is stronger than that of MeOH. The affinity between POSS and DMC is stronger than that of MeOH because of the hydrophobic vinyl on the surface of POSS particles. Therefore, DMC that passed through the membrane increased faster than MeOH because of the chemical potential on both sides of the membrane; therefore, the diffusivity increased. Diffusivity represents the trend of dynamic selectivity.

We found that the sorptivity of PDMS/POSS active layer did not change remarkably but the diffusivity decreased considerably with increasing temperature because, the saturated vapor pressure of MeOH increased faster with increasing temperature, and the difference in chemical potential on both sides was greater than that of DMC, which means that the driving force MeOH through the membrane surface increased more. The increase in temperature accelerates the movement of polymer chain segment inside the membrane and speeds up the molecular movement speed of MeOH and DMC. The molecular volume of MeOH is smaller, so it is easier to pass through the membrane and enter the downstream at lower temperatures; hence, the diffusivity decreased. However, sorptivity was less affected by similar effects, and the change was not obvious.

Comparison of sorptivity and diffusivity showed that the sorptivity factor  $\alpha_S$  of PDMS/POSS active layer is much larger than that of diffusivity factor  $\alpha_D$ , which shows that the diffusion speed of DMC and MeOH in PDMS/POSS active layer has little difference (Fig. 9). PDMS/POSS active layer for the whole PV separation process of DMC/MeOH system had more selective separation ability depending on the swelling selectivity, that is, the difference in thermodynamic equilibrium between

DMC and MeOH molecules dissolved into the membrane body. DMC is more likely to enter the PDMS/POSS active layer inside the membrane, selectively penetrate the membrane, and achieve separation.

**Table 2.** Comparison with the separation ability of DMC/MeOH mixture PV membranes in the literature

| Membrane                                | DMC content (wt. %) | T (°C) | Flux(K gm <sup>-2</sup> h <sup>-1</sup> ) | Preferential penetration | Separation factor | Reference |
|---|---------------------|--------|---|--------------------------|-------------------|-----------|
| CS                                      | 30                  | 55     | 0.27                                      | MeOH                     | 10                | 17        |
| PAA/PVA (7: 3)                          | 30                  | 60     | 0.58                                      | MeOH                     | 13                | 8         |
| PAA/PVA (6: 4)                          | 30                  | 60     | <0.6                                      | MeOH                     | <9                | 8         |
| PAA/PVA                                 | 30                  | 70     | 0.25                                      | MeOH                     | 37                | 26        |
| ZSM-5- CS (5: 95)                       | 30                  | 25     | 0.49                                      | MeOH                     | 4.5               | 27        |
| ZSM-5- CS (15: 85)                      | 30                  | 25     | 0.69                                      | MeOH                     | 2.8               | 27        |
| CS- SiO <sub>2</sub>                    | 30                  | 50     | 1.28                                      | MeOH                     | 29.8              | 28        |
| CSHollow Fiber                          | 30                  | 50     | 0.42                                      | MeOH                     | <6                | 29        |
| Perfluoro-Ion-Exchange                  | 30                  | 40     | 3.40                                      | MeOH                     | 2.5               | 31        |
| PVA-PFSA/PAN                            | 30                  | 50     | 0.18                                      | MeOH                     | 3                 | 32        |
| Crosslinked- CS                         | 30                  | 55     | 0.5                                       | MeOH                     | 7                 | 41        |
| Vi-PDMS-PHMS                            | 30                  | 40     | <2.00                                     | DMC                      | <5                | 34        |
| DNS-SiO <sub>2</sub> - Vi-PDMS-PHMS     | 30                  | 40     | <1.00                                     | DMC                      | <4                | 34        |
| Hydrophobic nano-SiO <sub>2</sub> /PDMS | 30                  | 40     | 0.70                                      | DMC                      | 4.0               | 35        |
| MCM-41-SiO <sub>2</sub> -PDMS           | 30                  | 40     | 0.90                                      | DMC                      | 3.8               | 36        |
| MCM-41SiO <sub>2</sub> -PDMS            | 30                  | 60     | 2.50                                      | DMC                      | 2.3               | 36        |
| PDMS-PVDF                               | 30                  | 40     | 0.49                                      | DMC                      | 3.9               | 12        |
| PDMS/POSSM-3                            | 30                  | 50     | 4.90                                      | DMC                      | 2.3               | This work |
| PDMS/POSSM-1                            | 30                  | 50     | 1.00                                      | DMC                      | 4.0               | This work |

#### 4. Conclusion

A new PV membrane with PAN as support layer was prepared by using vinyl POSS to modify PDMS and was used to separate DMC/MeOH azeotropic mixture preferentially through DMC. XRD and SEM images show that POSS affects the ordered structure of PDMS, and the highly crystalline cage structure of POSS is still retained. We evaluated the PV performance of PDMS/POSS composite membrane through the PV experiment of DMC/MeOH azeotropic mixture. The permeation flux of DMC increased gradually whereas the separation factor decreased with increasing POSS content in the composite membrane. The cage structure of POSS and the interaction between hydrophobic groups on the surface and PDMS affected the PV process. Results combined with the analysis of swelling selectivity and diffusion selectivity by swelling test revealed that the swelling selectivity of

permeable components entering into the active layer plays a more important role in the selectivity of the whole active layer in the separation process. PDMS/POSS composite membrane M-3 reached the maximum permeation flux of 4.9 kg/m<sup>2</sup>h at the operating temperature of 50 °C and has a separation factor of 2.31. The total DMC passing efficiency is higher than that reported in the literature (Table 2). The composite membrane has the potential for industrial application of PV in DMC/MeOH azeotropic mixture. At 30 °C, the maximum separation factor of PDMS/POSS composite membrane M-1 was 4.04 and the permeation flux was 1.0 kg/m<sup>2</sup>h. The PV of DMC/MeOH azeotropic mixture in the literature has a certain degree of improvement compared with the data of DMC. The results also show that regular nano silica particles with special functional groups and specific structures (such as POSS) can be introduced into the PV industry to produce composite membranes and thus expands the new membrane manufacturing methods in the field of PV.

### Acknowledgments

This work was respectively supported by University Natural Science Research Project of Anhui Province (No. KJ2019A0829) and Hefei University Science and Technology Development Foundation (No. 19ZR08ZDA).

### References

- [1] Arayaphan J., Boonsuk P., Chantarak S. (2020), Enhancement of water barrier properties of cassava starch-based biodegradable films using silica particles. *Iranian Polymer Journal*, **29**, 749-757.
- [2] Brown D., Neyertz S., Raaijmakers M.J.T. (2019), Sorption and permeation of gases in hyper-cross-linked hybrid poly(POSS-imide) networks: An in silico study, *Journal of Membrane Science*, **577**, 113-128.
- [3] Liu Y., Fan L., Pang J. (2020), Effect of tensile action on retrogradation of thermoplastic cassava starch/nanosilica composite, *Iranian Polymer Journal*, **29**(2), 171-183.

- [4] Chen D., Yi S., Wu W. (2010), Synthesis and characterization of novel room temperature vulcanized (RTV) silicone rubbers using Vinyl-POSS derivatives as cross linking agents, *Polymer* **51**.17, 3867-3878.
- [5] Chen D., Nie J., Yi S. (2010), Thermal behaviour and mechanical properties of novel RTV silicone rubbers using divinyl-hexa[(trimethoxysilyl)ethyl]-POSS as cross-linker, *Polymer Degradation and Stability*, **95**.4, 618-626.
- [6] Gupta K.M., Liu J., Jiang J. (2019), A molecular simulation protocol for membrane pervaporation. *Journal of Membrane Science*, 572, 676-682.
- [7] León J.A, Fontalvo J. (2019), PDMS modified membranes by 1-dodecanol and its effect on ethanol removal by pervaporation, *Separation and Purification Technology*, **210**, 364-370.
- [8] Chaudhari S., Kwon Y.S., Shon M.Y. (2019), Stability and pervaporation characteristics of PVA and its blend with PVAm membranes in a ternary feed mixture containing highly reactive epichlorohydrin, *RSC Advances*, **9**(11), 5908-5917.
- [9] Mutlu H., Ruiz J., Solleder S.C. (2012),: TBD Catalysis with Dimethyl Carbonate: A Fruitful and Sustainable Alliance, *Green Chemistry*, **14**.6, 1728-1735.
- [10] Tundo P., Memoli S., Rault D.H. (2004), Synthesis of methylethers by reaction of alcohols with dimethylcarbonate, *Green Chemistry*, **6**.12, 609-612.
- [11] Ono Y. (1996), Dimethyl carbonate for environmentally benign reactions, *Pure and Applied Chemistry*, **68**.2, 367-375.
- [12] Zhou H., Lv L., Liu G. (2014), PDMS/PVDF composite pervaporation membrane for the separation of dimethyl carbonate from a methanol solution, *Journal of Membrane Science*, **471**, 47-55.

- [13] Rakshit S., Saha R., Singha A. (2013), Molecular interaction, co-solubilization of organic pollutants and ecotoxicity of a potential carcinogenic fuel additive MTBE in water, *Journal of Molecular Liquids*, **180.3**, 235-243.
- [14] Rossner A., Knappe D.R.U. (2008), MTBE adsorption on alternative adsorbents and packed bed adsorber performance, *Water Research*, **42.8-9**, 2287-2299.
- [15] Takeuchi S., Fukutsuka T., Miyazaki K. (2013), Electrochemical lithium ion intercalation into graphite electrode in propylene carbonate-based electrolytes with dimethyl carbonate and calcium salt, *Journal of Power Sources*, **238**, 65-68.
- [16] Huang S., Yan B., Wang S. (2015), Recent advances in dialkyl carbonates synthesis and applications, *Chemical Society Reviews*, **44.10**, 3079-3116.
- [17] Won W., Feng X., Lawless D. (2002), Pervaporation with chitosan membranes: Separation of dimethyl carbonate/methanol/water mixtures, *Journal of Membrane Science*, **209.2**, 493-508.
- [18] Lin H., Yang B., Sun J. (2004), Kinetics studies for the synthesis of dimethylcarbonate from urea and methanol, *Chemical Engineering Journal*, **103**, 21-27.
- [19] Cai Q.H., Lu B., Guo L.J. (2009), Studies on synthesis of dimethyl carbonate from methanol and carbon dioxide, *Catalysis Communications*, **10.5**, 605-609.
- [20] Bian J., Xiao M., Wang S.J. (2009), Highly effective synthesis of dimethyl carbonate from methanol and carbon dioxide using a novel copper-nickel /graphite bimetallic nanocomposite catalyst, *Chemical Engineering Journal*, **147.2/3**, 287-296.
- [21] Tsuru T., Sasaki A., Kanazashi M. (2011), Pervaporation of methanol/dimethyl carbonate using SiO<sub>2</sub> membranes with nano - tuned pore sizes and surface chemistry, *AIChE Journal*, **57**, 2079-2089.
- [22] Romano U. (1976), Recovery of dimethyl carbonate from its azeotropic mixture with methanol, *DE Patent*, **2,607,003**.

- [23] Rechner J., Klausener A., Buysch H.J., Wagner P. (1993), Process for the preparation of dialkyl carbonates, *US Patent*, **5,274,163**.
- [24] Passoni G.A. (1973), Purification of dimethyl carbonate, *DE Patent*, **2,450,856**.
- [25] Chen J.H., Liu Q.L., Zhu A.M. (2008), Pervaporation separation of MeOH/DMC mixtures using STA/CS hybrid membranes, *Journal of Membrane Science*, **315**.1/2, 74-81.
- [26] Wang L., Li J., Lin Y. (2009), Crosslinked poly (vinyl alcohol) membranes for separation of dimethyl carbonate/methanol mixtures by pervaporation, *Chemical Engineering Journal*, **146**.1, 71-78.
- [27] Liu B., Cao Y., Wang T. (2007), Preparation of novel ZSM-5 zeolite-filled chitosan membranes for pervaporation separation of dimethyl carbonate/methanol mixtures, *Journal of Applied Polymer Science*, **106**.3, 2117-2125.
- [28] Chen J.H., Liu Q.L., Fang J. (2007), Composite hybrid membrane of chitosan–silica in pervaporation separation of MeOH/DMC mixtures, *Journal of Colloid and Interface Science*, **316**.2, 580-588.
- [29] Xiao T., Xu X., Cao Y. (2010), Preparation of asymmetric chitosan hollow fiber membrane and its pervaporation performance for dimethyl carbonate/methanol mixtures, *Journal of Applied Polymer Science*, **115**.5, 2875-2882.
- [30] Kope R., Meller M., Kujawski W. (2013), Polyamide-6 based pervaporation membranes for organic–organic separation, *Separation and Purification Technology*, **110**, 63-73.
- [31] Lang W.Z., Niu H.Y., Liu Y.X. (2013), Pervaporation separation of dimethyl carbonate/methanol mixtures with regenerated perfluoro - ion - exchange membranes in chlor - alkali industry, *Journal of Applied Polymer Science*, **129**.6, 3473-3481.
- [32] Niu H.Y., Lang W.Z., Liu Y.X. (2013), Pervaporation separation of dimethyl carbonate/methanol binary mixtures with poly (vinyl alcohol)-perfluorsulfonic

acid/poly(acrylonitrile) hollow fiber composite membranes, *Fiber and Polymer*, **14**.10, 1587-1594.

- [33] Stephenson R.M., Malanowski S. (1987), Handbook of the Thermodynamics of Organic Compounds, *Elsevier*, New York.
- [34] Wang L., Han X., Li J. (2011), Separation of Azeotropic Dimethylcarbonate/Methanol Mixtures by Pervaporation: Sorption and Diffusion Behaviors in the Pure and Nano Silica Filled PDMS Membranes, *Separation Science and Technology*, **46**.9, 1396-1405.
- [35] Wang L., Han X., Li J. (2011), Hydrophobic nano-silica/polydimethylsiloxane membrane for dimethylcarbonate-methanol separation via pervaporation, *Chemical Engineering Journal*, **171**.3, 1035-1044.
- [36] Wang L., Han X., Li J. (2013), Modified MCM - 41 silica spheres filled polydimethylsiloxane membrane for dimethylcarbonate/methanol separation via pervaporation, *Journal of Applied Polymer Science*, **127**.6, 4662-4671.
- [37] Zhang L., Yu P., Luo Y. (2007), Dehydration of caprolactam-water mixtures through cross-linked PVA composite pervaporation membranes, *Journal of Membrane Science*, **306**.1/2, 93-102.
- [38] Uragami T., Tsukamoto K., Inui K. (1998), Pervaporation characteristics of a benzoylchitosan membrane for benzene-cyclohexane mixtures, *Macromolecular Chemistry and Physics*, **199**.1, 49-54.
- [39] Zhou Y., Wu J.T., Lemmon E.W. (2011), Thermodynamic Properties of Dimethyl Carbonate. *Journal of Physical and Chemical Reference Data*, **40**.4, 043106/1-11.
- [40] Gibbard., Frank H., Creek., Jefferson L. (1974), Vapor pressure of methanol from 288.15 to 337.65.deg.K, *Journal of Chemical & Engineering Data*, **19**.4, 308-310.



- [41] Won W., Feng X., Lawless D. (2003), Separation of dimethyl carbonate/methanol/water mixtures by pervaporation using crosslinked chitosan membranes, *Separation and Purification Technology*. **31.2**, 129-140.

ACCEPTED MANUSCRIPT